Supplementary information

Electrospun carbon nanofibers with MnS sulfiphilic sites as an efficient polysulfide barrier for high performance wide temperature range Li-S batteries

Xin Wang,[a] Xiaosen Zhao,[a] Chenhui Ma,[a] Zhenzhen Yang,[a,d] Gang Chen,[a] Lei Wang,[b] Huijuan Yue,[c] Dong Zhang,*[a] , Zhenhua Sun*[d]

[a] *Key Laboratory of Physics and Technology for Advanced Batteries (Ministry of Education), Jilin Key Engineering Laboratory of New Energy Materials and Technologies, College of Physics, Jilin University, Changchun 130012, PR China*

[b] *Key Laboratory of Eco-Chemical Engineering (Ministry of Education), College of Chemistry and Molecular Engineering, Qingdao University of Science and Technology, Qingdao 266042, PR China*

[c] *State Key Laboratory of Inorganic Synthesis and Preparative Chemistry, College of Chemistry, Jilin University, Changchun 130012, PR China*

[d] *Shenyang National Laboratory for Materials Science, Institute of Metal Research, Chinese Academy of Sciences, Shenyang 110016, PR China*
E-mail: dongzhang@jlu.edu.cn (D. Zhang); zhsun@imr.ac.cn (Z. H. Sun)

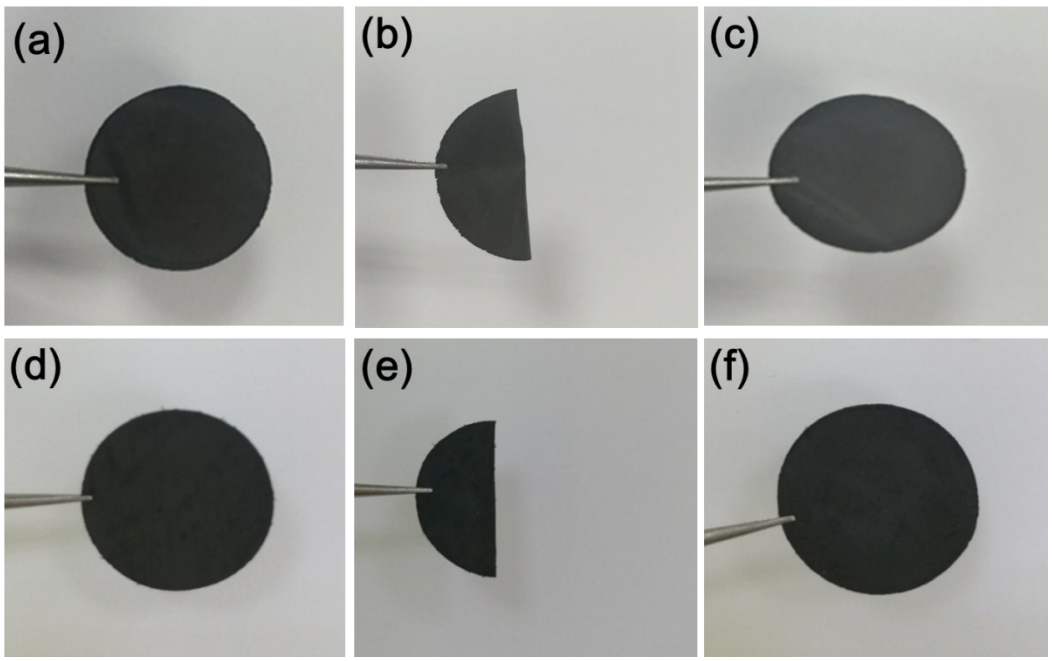

Fig. S1 Photographs of the CNFs interlayer (a) original, (b) folding and (c) after folding. Photographs of the MnS/CNFs interlayer (d) original, (e) folding and (f) after folding.

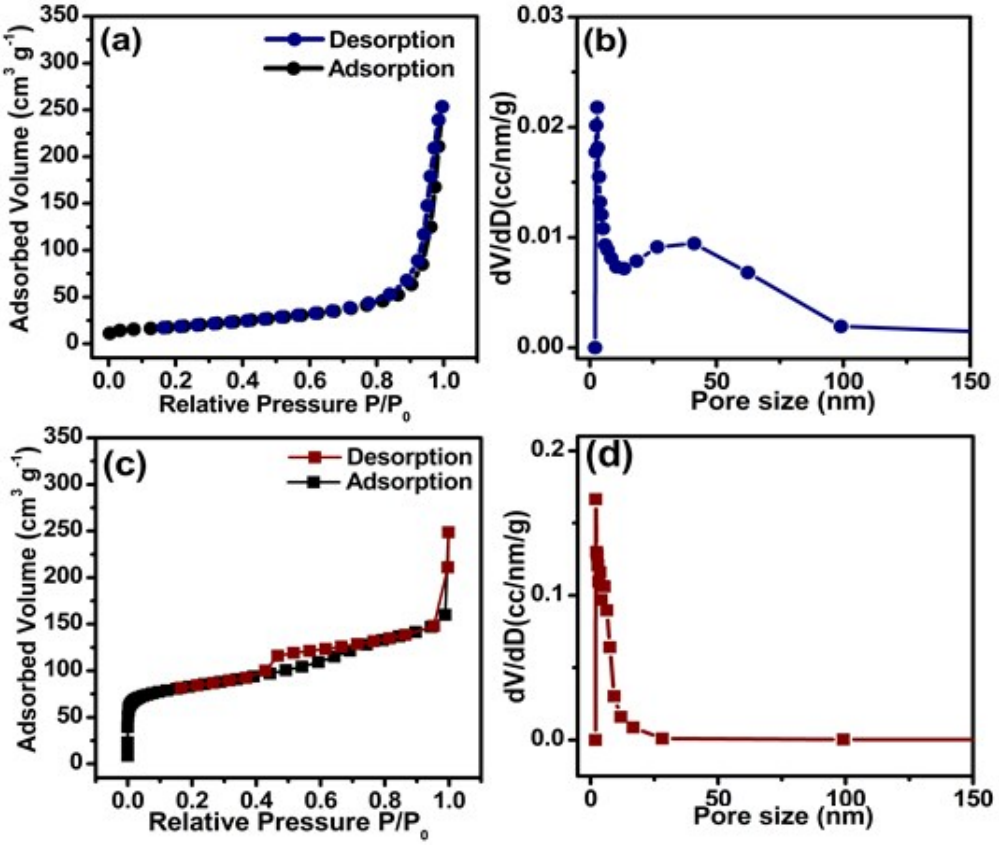

Fig. S2 (a) N_2 sorption isotherms and (b) pore-size distribution of CNFs interlayer. (c) N2 sorption isotherms and (d) pore-size distribution of MnS/CNFs interlayer.

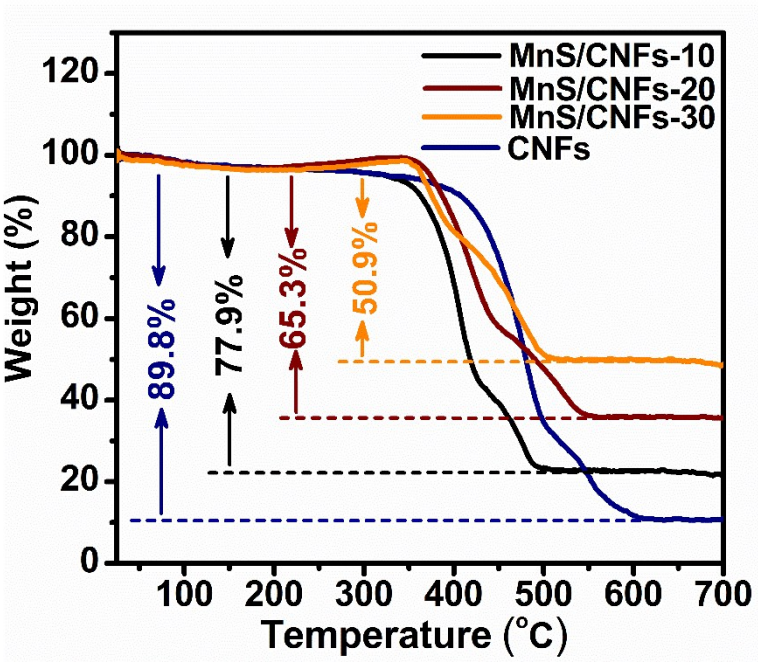

Fig. S3 TG curves of MnS/CNFs-10, MnS/CNFs-20, MnS/CNFs-30 and CNFs interlayers, respectively.

During the thermogravimetric test, the MnS particles in the MnS/CNFs interlayer react with oxygen to form Mn_2O_3 precipitate and SO_2 gas. As can be seen from the Fig. S3, the content of Mn_2O_3 is 24.5 wt.%. Therefore, the content of MnS in the MnS/CNFs-20 interlayer can be estimated to be 27.2 wt.% according to the following reaction equation.[1-3]

$$4MnS + 7O_2 \rightarrow 2Mn_2O_3 + 4SO_2$$

Molar mass： 174 157.8

Weight ratio： M_1 24.5 wt.%

M_1=24.5 wt.%÷157.8×174=27.2 wt.%

Similarly, the content of MnS in MnS/CNFs-10 and MnS/CNFs-30 interlayer was calculated to be 13.1 wt.% and 42.89 wt.%, respectively.

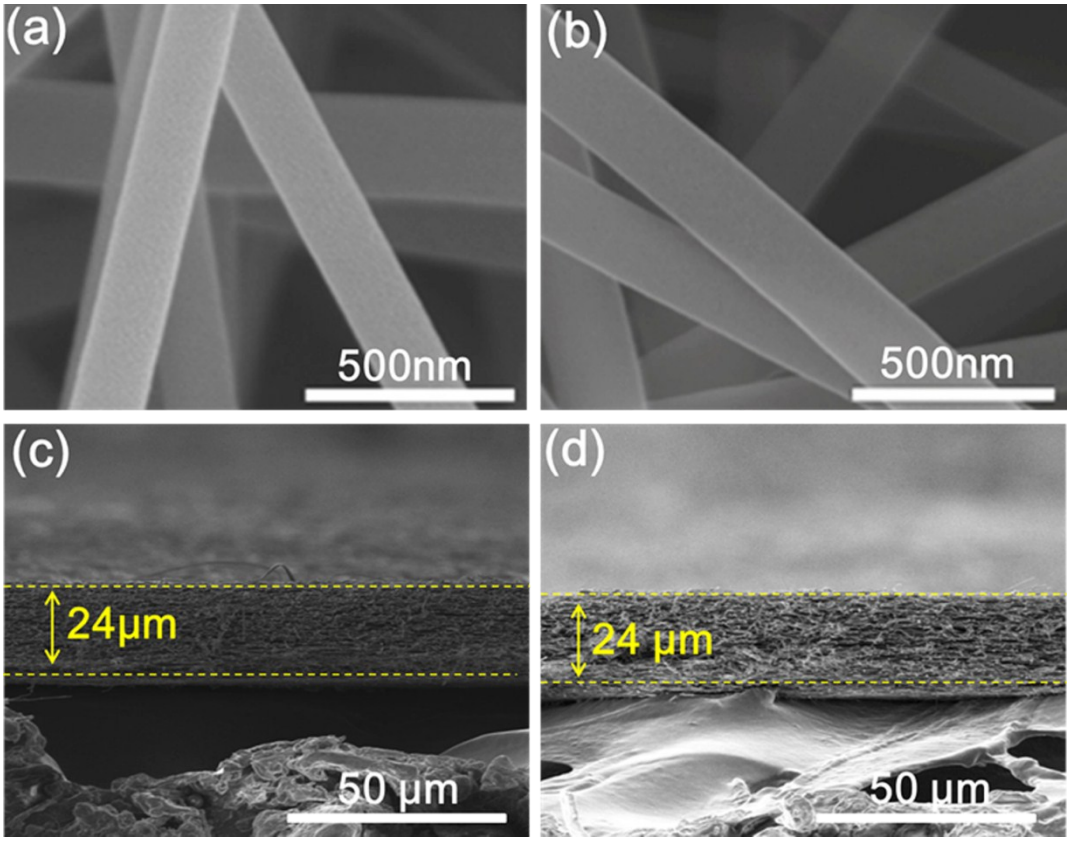

Fig. S4 High magnification SEM image of (a) CNFs interlayer and (b) MnS/CNFs interlayer. Cross-sectional SEM images of (c) CNFs interlayer and (d) MnS/CNFs interlayer.

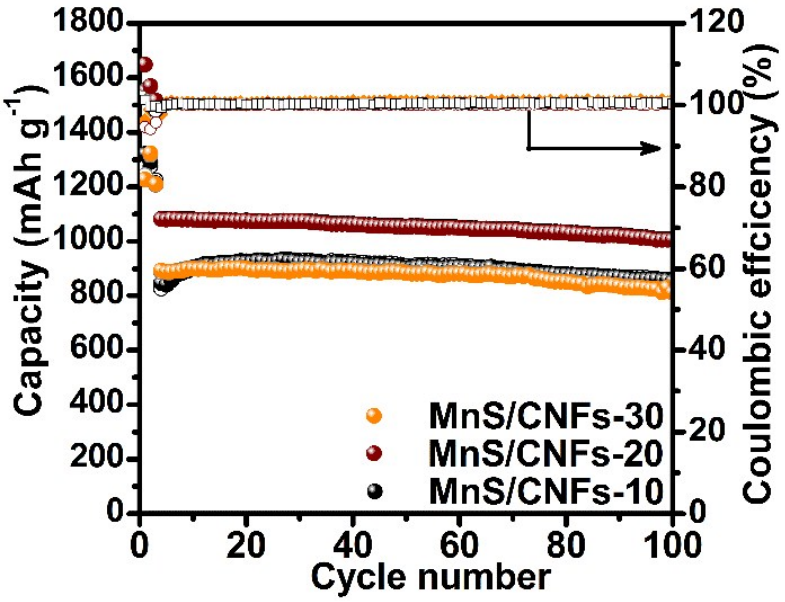

Fig. S5 Cycling performance of the cells with MnS/CNFs-10, MnS/CNFs-20 and MnS/CNFs-30 interlayers at 0.5 C, respectively.

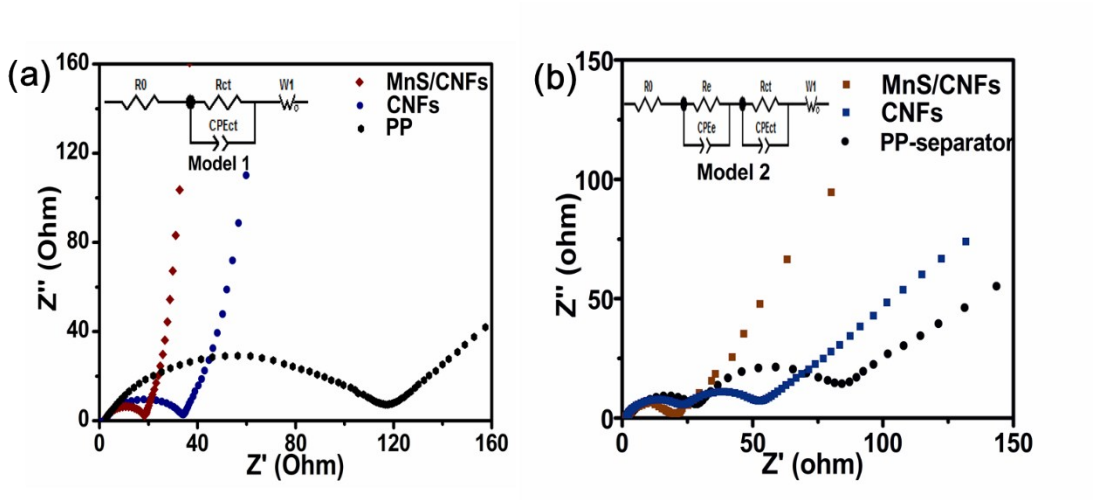

Fig. S6 Electrochemical impedance spectra of the cells with MnS/CNFs interlayer, CNFs interlayer and PP-separator (a) before cycles and (b) after 100 cycles, respectively.

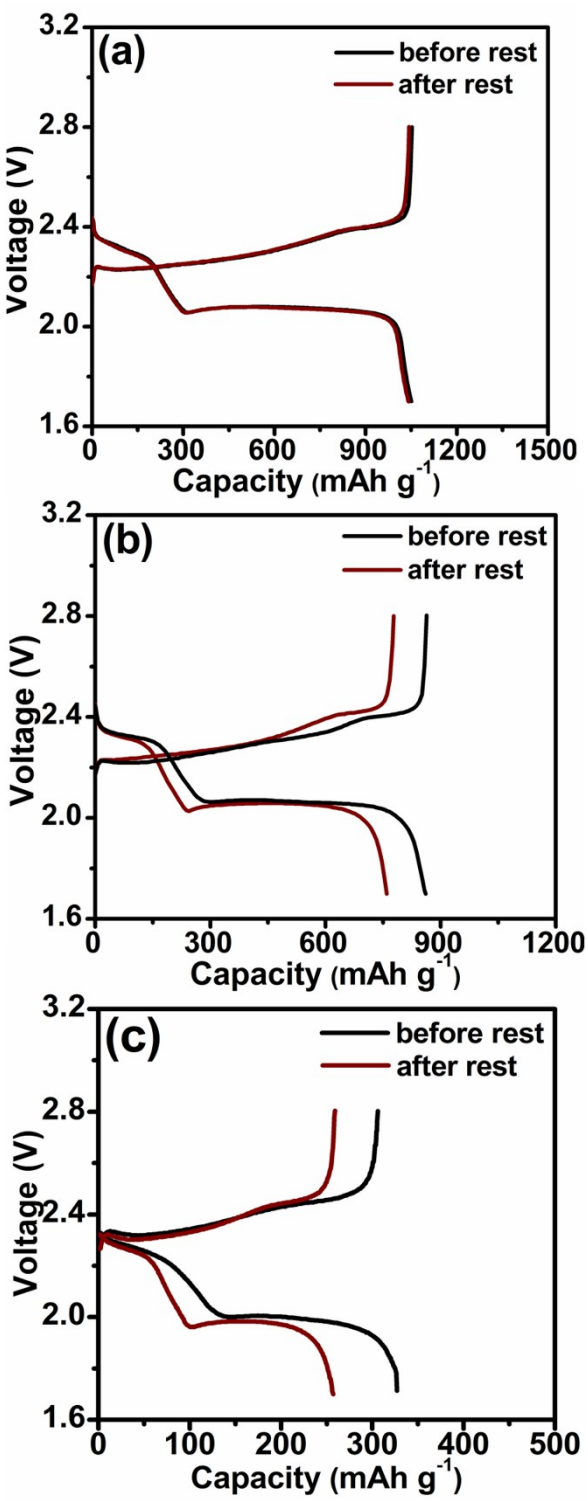

Fig. S7 Charge-discharge curves of cells with (a) MnS/CNFs interlayer, (b) CNFs interlayer and (c) PP-separator before and after 150 h rest.

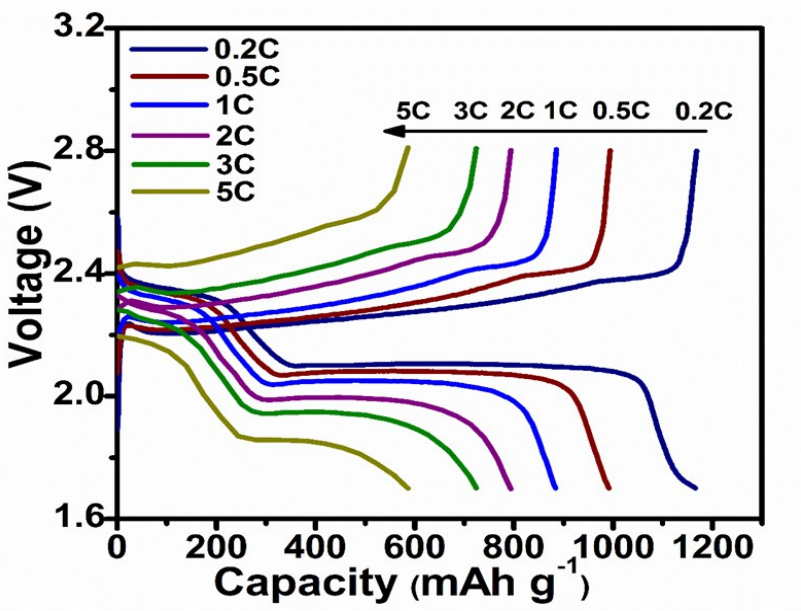

Fig. S8 Charge-discharge curves of cells with MnS/CNFs interlayer at different rates from 0.2 to 5 C.

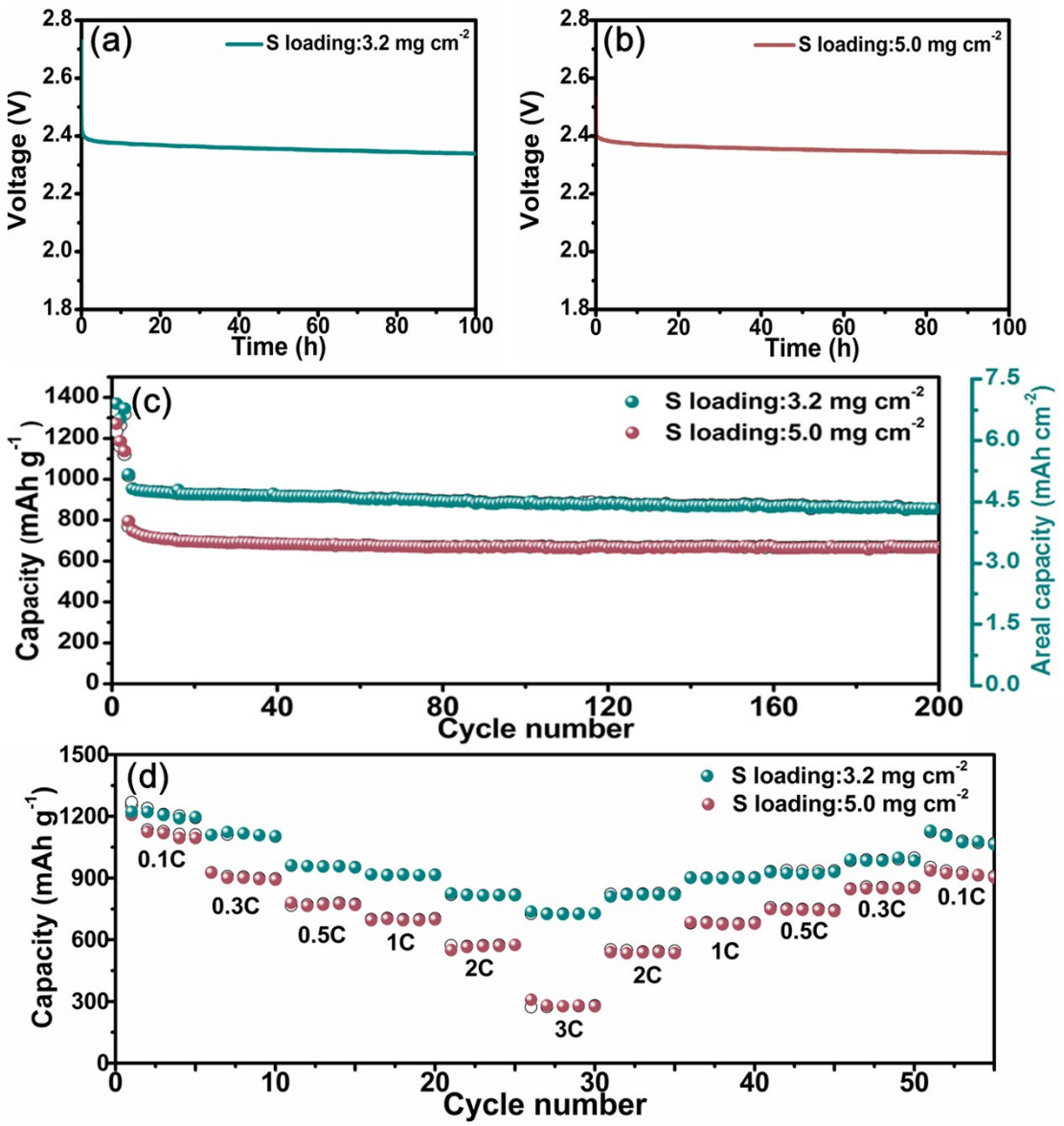

Fig. S9 The open-circuit voltage curves of the cells with MnS/CNFs interlayer with high sulfur loading cathodes of (a) 3.2 and (b) 5.0 mg cm^{-2} during 100 hours resting. (c) Cycling performance of cells with the MnS/CNFs interlayer with high sulfur loading cathodes of 3.2 and 5.0 mg cm^{-2} at 0.5 C, respectively. (d) Rate performances of cells with the MnS/CNFs interlayer with high sulfur loading cathodes of 3.2 and 5.0 mg cm^{-2}, respectively.

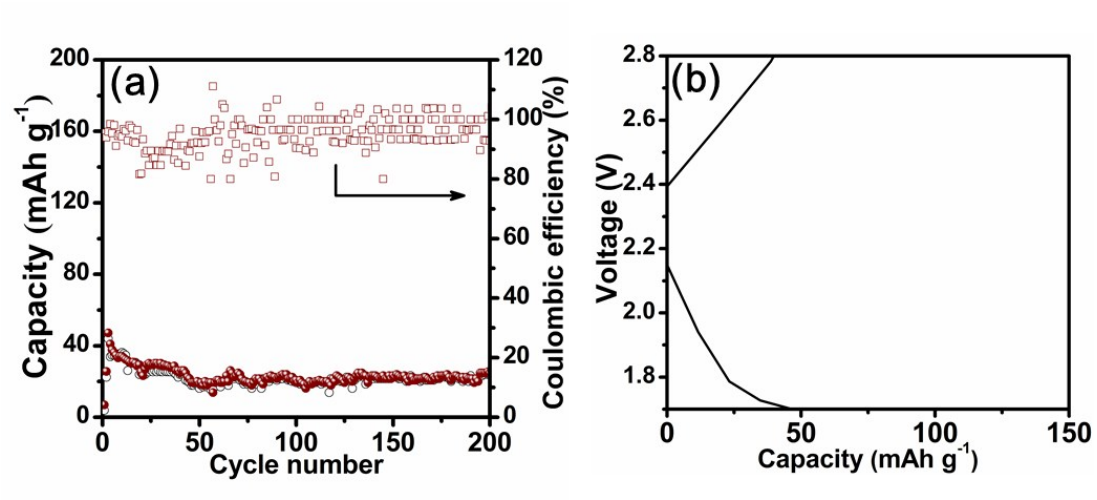

Fig. S10 (a) Electrochemical performance and (b) charge-discharge curve of MnS/CNFs as cathode. The pure MnS/CNFs interlayer shows a capacity of < 40 mAh g^{-1} in the voltage range of 2.8-1.7 V.

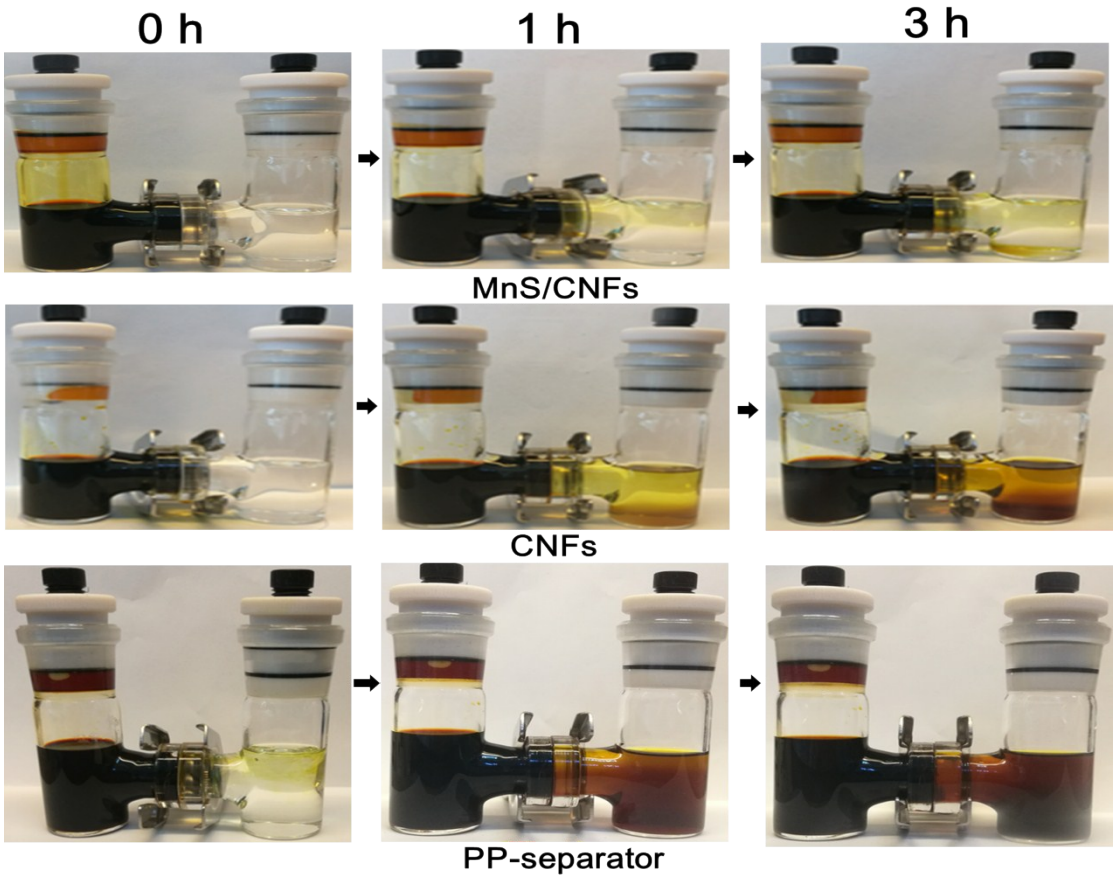

Fig. S11 Photographs of the LiPSs permeability tests for 0, 1 and 3 h with the MnS/CNFs, CNFs interlayer and PP-separator.

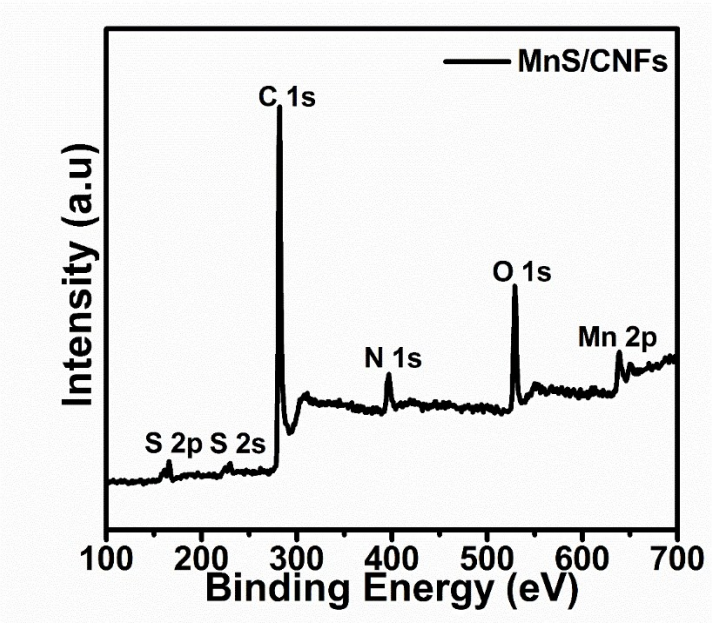

Fig. S12 Full XPS spectrum of the MnS/CNFs interlayer.

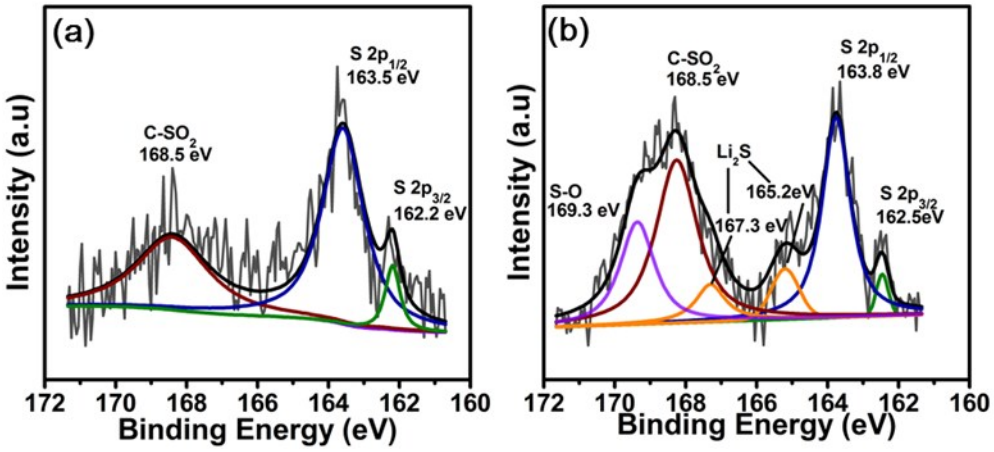

Fig. S13 The S 2p spectra of the MnS/CNFs interlayer (a) before and (b) after cycles.

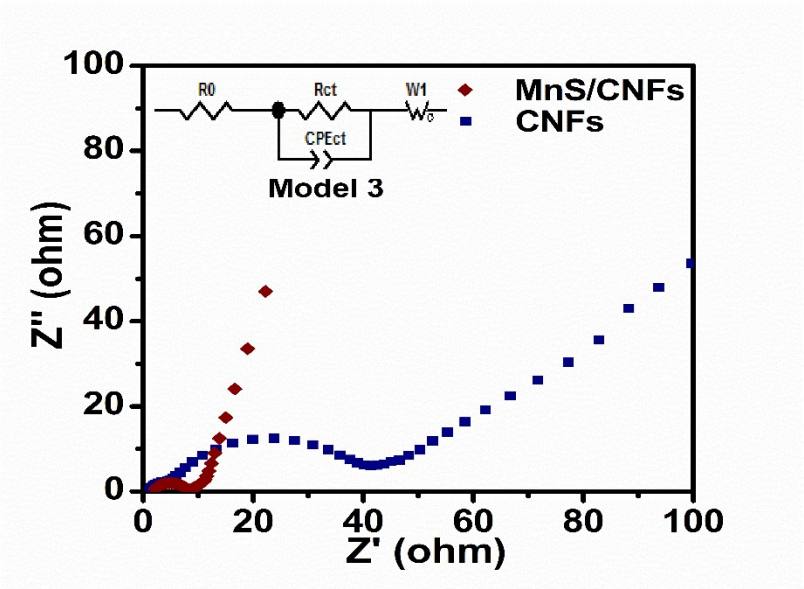

Fig. S14 Electrochemical impedance spectra of the cells with MnS/CNFs and CNFs interlayer after cycles under 55 °C.

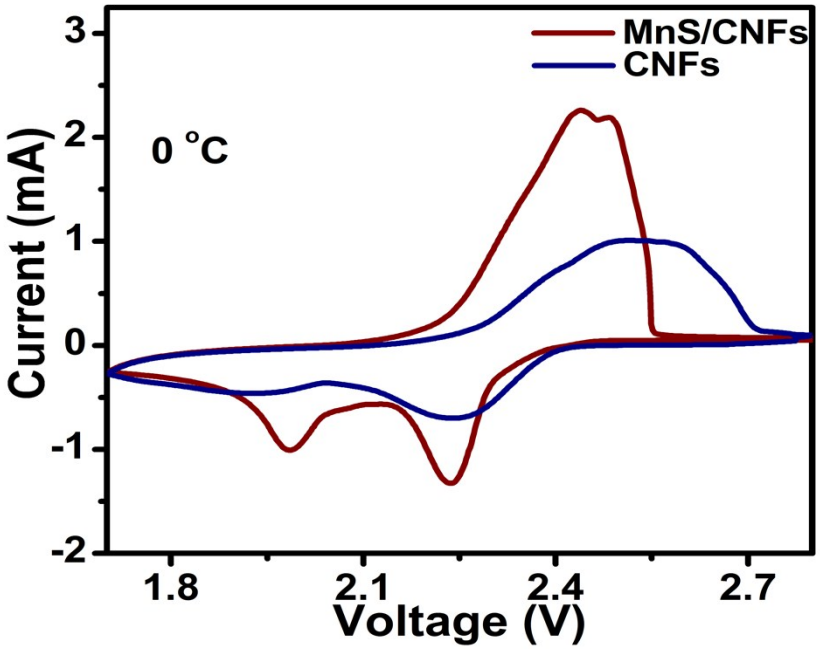

Fig. S15 CV curves of the cells with MnS/CNFs interlayer and CNFs interlayer at first cycle under 0 °C.

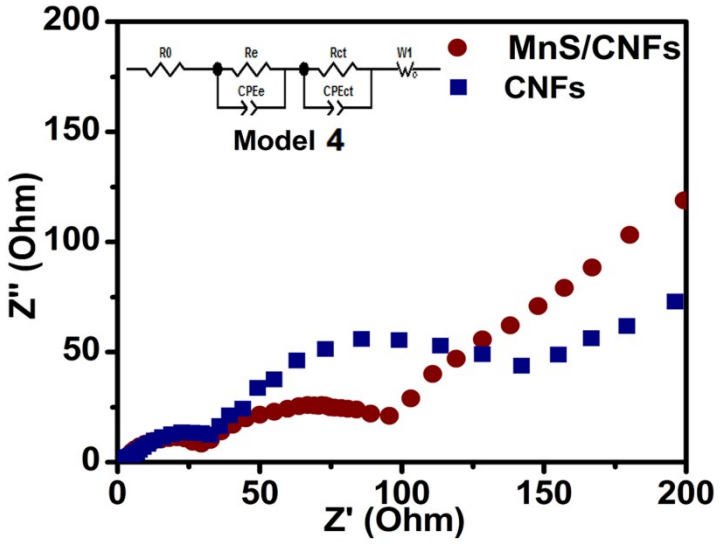

Fig. S16 Electrochemical impedance spectra of the cells with MnS/ CNFs and CNFs interlayer after cycles under 0 ^{o}C.

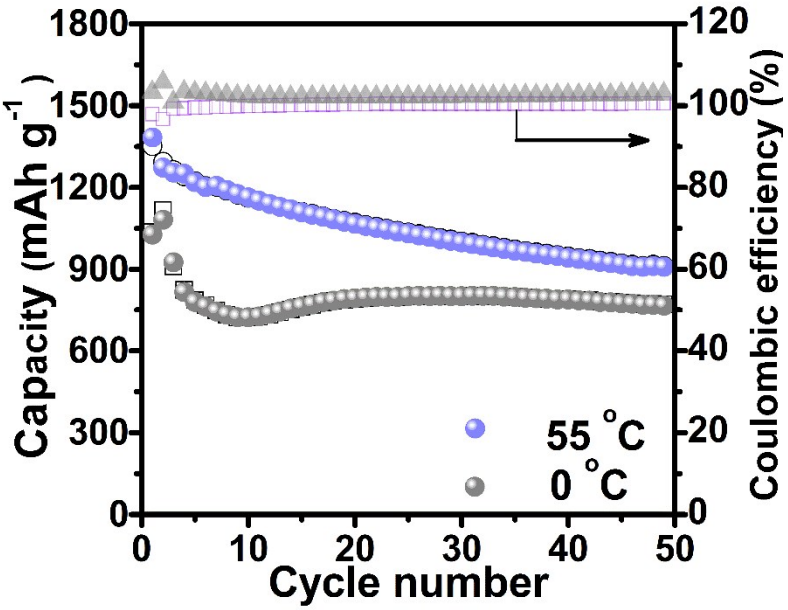

Fig. S17 Cycling performance of cells with the MnS/CNFs interlayer with high sulfur loading cathodes of 3.2 mg cm^{-2} at 0.5C under 55 °C and 0 °C, respectively.

Table S1 Impedance parameters calculated according to the equivalent circuits.

Samples	R_0 (Ω)	Rct (Ω)
Pristine	2.87	114.73
CNFs	1.42	37.28
MnS/CNFs	1.94	16.89

Table S2 Electrical conductivity of interlayers.

Samples	CNFs	MnS/CNFs-10	MnS/CNFs-20	MnS/CNFs-30
Electrical conductivity (S m^{-1})	19.11	18.53	17.19	15.25

Table S3 Performances comparison of this work with previous works using the interlayer for Li-S batteries.

Coating or interlayer	Area weight of sulfur (mg cm^{-1})	Current rate	Discharge capacities (mAh g^{-1}) and (cycle number)	Rate capacity (mAh g^{-1})	Ref
Silk fibroin nanofiber film	2.0	0.2C	700 (200)	670 (2C)	[4]
CNT@TiO_2 interlayer	~ 1.7	0.5C	541 (1000)	809 (2C)	[5]
Interwoven MoO_3@CNT scaffold	1.0	0.3C	755 (200)	655 (3C)	[6]
rGO@MoS_2 interlayer	1.8-2.0	0.2C 1C	671 (200) 368 (500)	615 (2C)	[7]
MoS_2 Nanosheets@N-Doped Carbon Interlayer	1.2	0.5C	880 (100)	876 (3C)	[8]

MnO_2/CNT/PP separator	0.8	0.5C 1C	670.9 (100) 573.7 (500)	794.5 (1C)	[9]
$BaTiO_3$-decorated carbon nanofbers	1	0.3C	865 (200)	672 (3C)	[10]
oPANVP/$SnCl_2$	3	0.2C	700 (100)	480 (1C)	[11]
MnS/CNFs interlayer	2 5	1C 0.5C	810 (400) 714(200)	586 (5C) 575 (2C)	This work

References

[1] K. M. Jeon, J. S. Cho and Y. C. Kang, *J. Power Sources*, 2015, **295**, 9-15

[2] X. Xu, S. Ji, M. Gu and J. Liu, *ACS Appl. Mater. Interfaces*, 2015, **7**, 20957-20964.

[3] S. Gao, G. Chen, Y. Dall'Agnese, Y. Wei, Z. Gao and Y. Gao, *Chem. Eur. J.*, 2018, **24**, 13535

[4] K. Wu, Y. Hu, Z. Cheng, P. Pan, L. Jiang, J. Mao, C. Ni, X. Gu, Z. Wang and *J. Membr. Sci.*, 2019, 592, 117349.

[5] L. Yang, G. Li, X. Jiang, T. Zhang, H. Lin and J. Y. Lee, *J. Mater. Chem. A*, 2017, 5, 12506-12512.

[6] L. Luo, X. Qin, J. Wu, G. Liang, Q. Li, M. Liu, F. Kang, G. Chen and B. Li, *J. Mater. Chem. A*, 2018, 6, 8612-8619.

[7] L. Tan, X. Li, Z. Wang, H. Guo, and J. Wang, *ACS Appl. Mater. Interfaces*, 2018, 10, 3707−3713.

[8] J. Wu, X. Li, H. Zeng, Y. Xue, F. Chen, Z. Xue, Y. Ye and X. Xie, *J. Mater. Chem. A*, 2019, 7, 7897.

[9] Y. Wang, W. Liu, R. Liu, P. Pan, L. Suo, J. Chen,X. Feng, X. Wang, Y. Ma and W. Huang, *New J. Chem.*, 2019, 43, 14708.

[10] S. Zhang, X. Qin, Y. Liu, L. Zhang, D. Liu, Y. Xia, H. Zhu, B. Li and F. Kang, *Adv. Mater. Interfaces*, 2019, 1900984.

[11] E. C. Cengiz, O. Ozturk, S. H. Soytas and R. Demir-Cakan, *J. Power Sources*, 2019, 412, 472.